COMMUNICATION www.rsc.org/chemcomm | ChemComm

The effect of molecular conformation on single molecule conductance: measurements of π-conjugated oligoaryls by STM break junction†

I-Wen Peter Chen,[a] Ming-Dung Fu,[a] Wei-Hsiang Tseng,[a] Chun-hsien Chen,*[b] Chih-Ming Chou[b] and Tien-Yau Luh*[b]

Received (in Cambridge, UK) 12th April 2007, Accepted 8th May 2007
First published as an Advance Article on the web 17th May 2007
DOI: 10.1039/b705521h

Measurements of molecular break junction reveal quantitatively the correlation betweeen the single-molecule conductance and the conformation of π-conjugated molecules with 6–18 conjugated double bonds.

Although the conformation of molecules has long been believed a major factor that influences the electron transporting properties,[1–6] only very recently, Venkataraman and co-workers first unveiled the effect of torsion angles on the conductance of biphenyls by constraining the dihedral angles between the neighboring aryl rings.[6] Unambiguous experimental findings associated with the deformation and stretching of π-conjugated molecules are yet unavailable because the studies of single-molecule conductance focus mostly on saturated alkane chains,[6–12] *para*-derivatized benzenes,[6,12–15] DNA oligonucleotides,[16,17] peptide,[18] rigid OPEs,[19] ligand-supported metal strings,[20,21] and short oligomers.[16,17] These model systems have either ill-conductive chains or rigid frameworks which do not yield a readily discernible correlation of the single-molecule conductance to the conformational stretching along the molecular long axis. Herein, we manifest this effect by designing conjugated and relatively flexible oligoaryls (Fig. 1) with alternating benzene–furan units, synthesized by the bidirectional iterative annulation protocol that allows precisely controllable conjugation length toward rationally tailored molecular wires.[22–24]

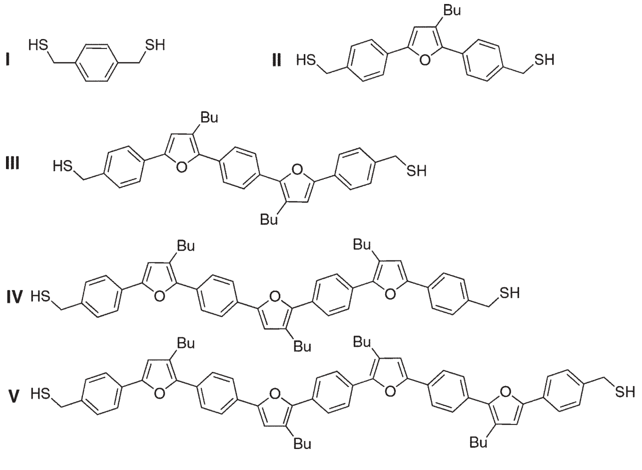

Fig. 1 Structures of thiolated benzene–furan oligoaryls.

The single-molecule junction conductance was measured by recording currents at a fixed bias voltage across a metal–molecule–metal assembly configured by STM break junction (scanning tunneling microscopy). The experimental procedures and data treatment are referred to the thorough account in literature.[6–8,18–20,25–29] Briefly, molecular junctions were repeatedly generated by bringing a gold STM tip into and out of contact (5–10 nm s^{-1}) with a gold substrate in toluene containing the compound (1 mM) of interest. When the STM tip was dipped onto the substrate, the current increased drastically, revealing that a point contact between the gold electrodes was created. During withdrawal of the tip, the gold contact was broken and a gold bridge was pulled out. The cross-section of the bridge was eventually thinning to that of a single strand of gold atoms and the gold chain was subsequently broken.[30] The corresponding conductance traces exhibited quantized steps which were integral multiples of the fundamental conductance, $G_o = 2e^2/h$ (~77.4 μS or $(12.9\ \mathrm{k\Omega})^{-1}$, where e is the electron charge and h is Planck's constant).[30] In the absence of molecules, the conductance traces showed exponential decay associated with the tip displacement, attributed to the tunneling event between the electrodes. Upon the formation of the tip–substrate gap in the presence of dithiol molecules, the thiol headgroups at the molecular termini might bind simultaneously onto the gold electrodes. The conductance traces responding to the tip withdrawn from the gold substrate (I(s) curves) appeared a stepwise and quantized fashion, suggesting the presence of integer numbers of molecules in between the junction. The I(s) profiles were recorded by a NanoScope built-in program and exported as ASCII files. Each trace had 5120 data points which were converted into conductance after being divided by the applied bias voltage. Experimental details by Tao and Lindsay[8,28] should be strictly followed to acquire better defined traces, in particular, by taking special care in the preparation of sharp tips and flat substrate.

The single-molecule resistance of compound **I** is 20.9 ± 2.9 MΩ, in a good agreement with 21 MΩ of the literature value.[13] For oligoaryls **II–V**, Panels (a)–(d) of Fig. 2 show their general I(s) features, significantly different than those of ill-conductive polymethylene chains[8,28] or rigid molecules.[20,28] For comparison, displayed in Fig. 2(e) and (f) are typical stepwise traces, respectively, for octanedithiol and a rigid metal string complex, $[Co_3(\mu_3\text{-dpa})_4(NCS)_2]$,[20] whose $I(s)$ traces comprise reasonably smooth and clean steps. Note that when the STM tip is pulled

---

[a] *Department of Chemistry, National Tsing Hua University, Hsinchu, 30013, Taiwan, Republic of China*
[b] *Department of Chemistry, National Taiwan University, Taipei, 10617, Taiwan, Republic of China. E-mail: chhchen@ntu.edu.tw; tyluh@ntu.edu.tw; Tel: +886 (2)33664191*

† Electronic supplementary information (ESI) available: Synthesis and H^1 NMR spectra of **II–V**, and X-ray structure of a **III** analogue (ORTEP). See DOI: 10.1039/b705521h

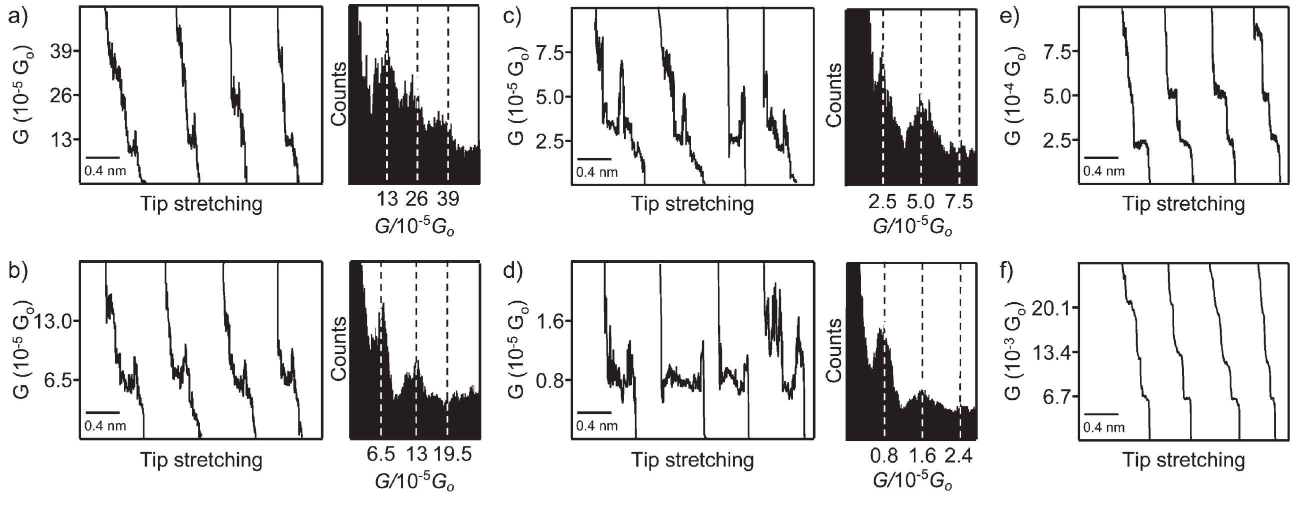

Fig. 2 Traces of conductance versus STM tip stretching and histograms measured by STM break junction. (a)–(d) **II**–**V**, (e) octanedithiol, (f) $[Co_3(\mu_3\text{-}dpa)_4(NCS)_2]$.[20] dpa^-, dipyridylamido anion; NCS, isothiocyanate. $G_o = 2e^2/h \sim 77.4$ μS, the fundamental conductance unit,[30] where *e* is the electron charge and *h* is the Planck's constant.

away from the substrate, the bridging molecule is concomitantly stretched out. For Compounds **II**–**V**, the *I*(*s*) steps appear extended longer than those in panels (e) and (f) (see Table 1), ascribed to the relatively long and flexible framework of the oligoaryls. More than one-third of the *I*(*s*) curves exhibits a peak near the step edge where the breakdown of the molecule-to-electrode contact takes place. At some point prior to the junction breakage, the molecule might develop a better conjugated conformation such as ideal bond angles and co-planarity which improve the π-electron propagating along the chain and should be accounted for the peaks in the *I*(*s*) traces. Note that nearly two-third of the *I*(*s*) traces do not exhibit isolated peaks. Regardless whether the isolated peak is present, all *I*(*s*) traces of Compounds **II**–**IV** fluctuate pronouncedly while those of rigid molecules appear smooth (*e.g.* Fig. 2(f)), providing a strong support for the correlation between the molecule conductance and the corresponding conformation.

Table 1 summarizes the single-molecule conductance for compounds **I**–**V**. Two types of conductance values, *G* and G_{peak}, are derived by the following manner. The former is decided by conductance histograms (Fig. 2(a)–(d)) which exclude *I*(*s*) traces with plainly tunneling decay to facilitate the determination of *G*.[28] G_{peak} is an average of the peak values measured curve by curve (at least 400 out of a total of more than 1200 traces for each compound). Accordingly, *G* and G_{peak} correspond to the most probable and the most conductive values of the molecules, respectively. Peaked *I*(*s*) profiles can actually be found in literature reports of STM break junction under toluene,[7,8,25–27,31] but was not subjected to discussion probably because of their relatively small magnitudes for alkanedithiols[25–27,31] or the statistically insignificant frequency.[28] Such ambiguity is less problematic in the present study of oligoaryls because the π-conjugated framework renders a pronounced $\Delta G/G$ ratio and because this *I*(*s*) behavior is well correlated to the systematically increased benzene–furan units of **II**–**V**. A longer benzene–furan oligoaryl confers a longer step (Δs in Table 1) and a larger $\Delta G/G$ ratio. Due to the flexible and conjugated framework, the ratio of $\Delta G/G$ for compound **V** reaches 75%, so distinct that the effect of tip stretching and consequently the molecular conformation must play a significant role.

Table 1 Conductance and ΔG/G of π-conjugated oligoaryls **I**–**V**

	n	$G/10^{-5}G_o$[a]	$G_{\text{peak}}/10^{-5}G_o$	$\Delta G/G$[c] (%)	Δs[d]/nm
I	0	62 ± 9	NA[b]	NA[b]	0.09 ± 0.05
II	1	13 ± 2	14.4 ± 2.5	11 ± 3	0.33 ± 0.11
III	2	6.5 ± 0.6	8.1 ± 1.4	25 ± 6	0.38 ± 0.12
IV	3	2.5 ± 0.2	3.6 ± 0.8	44 ± 14	0.47 ± 0.14
V	4	0.8 ± 0.1	1.4 ± 0.2	75 ± 18	0.57 ± 0.19

[a] $G_o \sim 77.4$ μS or (12.9 kΩ)$^{-1}$. [b] Not available. [c] $\Delta G = G_{\text{peak}} - G$, where *G* was obtained from all traces except those exhibiting simple exponential decay and G_{peak} was averaged from those with a peak near the end of the step. [d] Δs: the extension of the step. The values of Δs should not be over-interpreted in a quantitative manner because Δs is notably affected by the ill-defined microscopic structure at the molecule junction.

The electronic decay constant, *β*,[32] is a measure of the degree that impedes electron transport through the molecule. *β* is derived from $G = A\exp(-\beta_n n)$, where *n* is the number of the repetitive units for a homologous series of molecules. The semi-logarithm plot of the conductance values against *n* shows respective β_n for *G* and G_{peak} of 0.93 (±0.02) and 0.77 (±0.01) per *n*, corresponding to *β* of 0.13 ± 0.01 and 0.11 ± 0.01 Å^{-1}, based on a linear distance of 7.4 Å for a benzene–furan unit (see ESI† for an ORTEP diagram of an analogue of **III**). For comparison, typical *β* values are ~0.8 Å^{-1} for alkyl chains.[7–12,28] The *β* values of **II**–**V** are small and comparable to those of neutral or one-electron oxidized carotenoid polyenes with, respectively, benzyl mercaptan (0.22 ± 0.04 Å^{-1})[26] or pyridine (0.11 ± 0.03 Å^{-1})[29] headgroups, demonstrating the good π-electron conjugation of the oligoaryls. The *β* extracted from G_{peak} is somewhat smaller than that from *G*, indicating that the tip stretching near the junction breakage renders a superior conjugated conformation to those with the most probable conductance.

Fig. 3 shows the plot of G_{peak} against the number of benzene–furan unit, *n*. The intercept of the semi-logarithm graph gives the pre-exponential factor, *A*, whose reciprocal corresponds to the apparent resistance at the molecule–electrode contact. Because

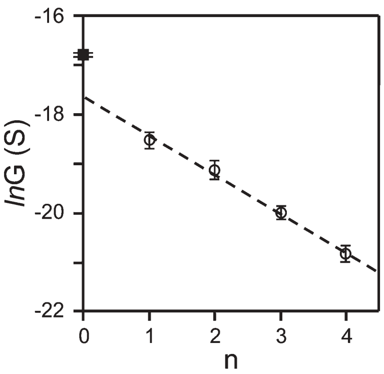

Fig. 3 Semi-logarithm plot of single-molecule conductance (ln G_{peak}) *vs.* *n* for the π-conjugated oligoaryls. Solid square: Compound **I**; open circles: benzene–furan oligoaryls, **II–V**.

the intercept for **II–V** represents an identical structure to that of **I** (see Fig. 1), it would seem that the contact resistance of the oligoaryls should be the same as the single-molecule junction resistance of **I**. Interestingly, the contact resistance of **II–V** is 38.7 ± 1.1 MΩ, almost two times the resistance of **I** (20.9 ± 2.9 MΩ). This discrepancy shows that the meta-molecule contact strength is, rather than a constant, weakened by the hybridization of the benzenedimethanethiol headgroup with the π-conjugated backbone.

In summary, with the relatively flexible benzene–furan oligoaryls, we demonstrate the effect of molecular conformation on the conductance of π-conjugated molecules. Upon the tip stretching, the conformations at G_{peak} develop a smaller β than those of the most probable G. The fact that the contact resistance of**II–V** is larger than the single-molecule resistance of **I** shows the importance of molecular backbone-headgroup interactions on the electron transmission probability through the headgroup.

The authors thank the National Science Council, the Ministry of Education (Taiwan, R.O.C), and College of Science (National Taiwan University) for financial support.

Notes and references

1 H. Basch, R. Cohen and M. A. Ratner, *Nano Lett.*, 2005, **5**, 1668–1675.
2 J. M. Seminario, C. E. De La Cruz and P. A. Derosa, *J. Am. Chem. Soc.*, 2001, **123**, 5616–5617.
3 M. P. Samanta, W. Tian, S. Datta, J. I. Henderson and C. P. Kubiak, *Phys. Rev. B*, 1996, **53**, R7626–R7629.
4 Z. J. Donhauser, B. A. Mantooth, K. F. Kelly, L. A. Bumm, J. D. Monnell, J. J. Stapleton, D. W. Price, Jr., A. M. Rawlett, D. L. Allara, J. M. Tour and P. S. Weiss, *Science*, 2001, **292**, 2303–2307.
5 W. Haiss, H. van Zalinge, D. Bethell, J. Ulstrup, D. J. Schiffrin and R. J. Nichols, *Faraday Discuss.*, 2006, **131**, 253–264.
6 L. Venkataraman, J. E. Klare, C. Nuckolls, M. S. Hybertsen and M. L. Steigerwald, *Nature*, 2006, **442**, 904–907.
7 S.-Y. Jang, P. Reddy, A. Majumdar and R. A. Segalman, *Nano Lett.*, 2006, **6**, 2362–2367.
8 X. Li, J. He, J. Hihath, B. Xu, S. M. Lindsay and N. Tao, *J. Am. Chem. Soc.*, 2006, **128**, 2135–2141.
9 M. Fujihira, M. Suzuki, S. Fujii and A. Nishikawa, *Phys. Chem. Chem. Phys.*, 2006, **8**, 3876–3884.
10 X. D. Cui, A. Primak, X. Zarate, J. Tomfohr, O. F. Sankey, A. L. Moore, T. A. Moore, D. Gust, G. Harris and S. M. Lindsay, *Science*, 2001, **294**, 571–574.
11 B. Xu and N. J. Tao, *Science*, 2003, **301**, 1221–1223.
12 J. Ulrich, D. Esrail, W. Pontius, L. Venkataraman, D. Millar and L. H. Doerrer, *J. Phys. Chem. B*, 2006, **110**, 2462–2466.
13 X. Xiao, B. Xu and N. J. Tao, *Nano Lett.*, 2004, **4**, 267–271.
14 L. Venkataraman, Y. S. Park, A. C. Whalley, C. Nuckolls, M. S. Hybertsen and M. L. Steigerwald, *Nano Lett.*, 2007, **7**, 502–506.
15 P. Reddy, S.-Y. Jang, R. A. Segalman and A. Majumdar, *Science*, 2007, **315**, 1568–1571.
16 H. van Zalinge, D. J. Schiffrin, A. D. Bates, E. B. Starikov, W. Wenzel and R. J. Nichols, *Angew. Chem., Int. Ed.*, 2006, **45**, 5499–5502.
17 H. van Zalinge, D. J. Schiffrin, A. D. Bates, W. Haiss, J. Ulstrup and R. J. Nichols, *ChemPhysChem*, 2006, **7**, 94–98.
18 X. Xiao, B. Xu and N. Tao, *Angew. Chem., Int. Ed.*, 2004, **43**, 6148–6152.
19 X. Xiao, L. A. Nagahara, A. M. Rawlett and N. Tao, *J. Am. Chem. Soc.*, 2005, **127**, 9235–9240.
20 I-W. P. Chen, M.-D. Fu, W.-H. Tseng, J.-Y. Yu, S.-H. Wu, C.-J. Ku, C.-h. Chen and S.-M. Peng, *Angew. Chem., Int. Ed.*, 2006, **45**, 5814–5818.
21 S.-Y. Lin, I-W. P. Chen, C.-h. Chen, M.-H. Hsieh, C.-Y. Yeh, T.-W. Lin, Y.-H. Chen and S.-M. Peng, *J. Phys. Chem. B*, 2004, **108**, 959–964.
22 C.-F. Lee, C.-Y. Liu, H.-C. Song, S.-J. Luo, J.-C. Tseng, H.-H. Tso and T.-Y. Luh, *Chem. Commun.*, 2002, 2824–2825.
23 C.-M. Chou, W.-Q. Chen, J.-H. Chen, C.-L. Lin, J.-C. Tseng, C.-F. Lee and T.-Y. Luh, *Chem. Asian J.*, 2006, **1**, 46–55.
24 S.-Y. Lin, I-W. P. Chen, C.-h. Chen, C.-F. Lee, C.-M. Chou and T.-Y. Luh, *J. Phys. Chem. B*, 2005, **109**, 7915–7922.
25 B. Xu, P. Zhang, X. Li and N. Tao, *Nano Lett.*, 2004, **4**, 1105–1108.
26 J. He, F. Chen, J. Li, O. F. Sankey, Y. Terazono, C. Herrero, D. Gust, T. A. Moore, A. L. Moore and S. M. Lindsay, *J. Am. Chem. Soc.*, 2005, **127**, 1384–1385.
27 B. Q. Xu, X. L. Li, X. Y. Xiao, H. Sakaguchi and N. J. Tao, *Nano Lett.*, 2005, **5**, 1491–1495.
28 F. Chen, X. Li, J. Hihath, Z. Huang and N. Tao, *J. Am. Chem. Soc.*, 2006, **128**, 15874–15881.
29 I. Visoly-Fisher, K. Daie, Y. Terazono, C. Herrero, F. Fungo, L. Otero, E. Durantini, J. J. Silber, L. Sereno, D. Gust, T. A. Moore, A. L. Moore and S. M. Lindsay, *Proc. Natl. Acad. Sci. USA*, 2006, **103**, 8686–8690.
30 H. Ohnishi, Y. Kondo and K. Takayanagi, *Nature*, 1998, **395**, 780–783.
31 K. Ishizuka, M. Suzuki, S. Fujii, Y. Takayama, F. Sato and M. Fujihira, *Jpn. J. Appl. Phys.*, 2006, **45**, 2037–2040.
32 D. M. Adams, L. Brus, C. E. D. Chidsey, S. Creager, C. Creutz, C. R. Kagan, P. V. Kamat, M. Lieberman, S. M. Lindsay, R. A. Marcus, R. M. Metzger, M. E. Michel-Beyerle, J. R. Miller, M. D. Newton, D. R. Rolison, O. Sankey, K. S. Schanze, J. Yardley and X. Zhu, *J. Phys. Chem. B*, 2003, **107**, 6668–6697.